

**A TEM STUDY OF PRISTINE MATRIX FROM THE TAGISH LAKE METEORITE.** A. Blinova<sup>1</sup>, T. J. Zega<sup>2</sup>, C. D. K. Herd<sup>1</sup>, and R. M. Stroud<sup>2</sup>. <sup>1</sup>Department of Earth and Atmospheric Sciences, 1-26 Earth Sciences Building, University of Alberta, Edmonton, AB, T6G 2E3, Canada ([blinova@ualberta.ca](mailto:blinova@ualberta.ca)), <sup>2</sup>Materials Science and Technology Division, Code 6366, Naval Research Laboratory, 4555 Overlook Ave. SW, Washington D.C., 20375.

**Introduction:** Tagish Lake is an ungrouped Type 2 carbonaceous chondrite (CC) with affinities to CIs and CMs [1,2]. In an effort to further characterize the Tagish Lake CC and understand its history, we initiated a mineralogical and petrological study of prominent macroscopic variations in pristine samples using electron microprobe, X-ray diffraction, and cathodoluminescence methods [3,4]. We identified four specimens that encompass varying degrees of aqueous alteration. For example, specimen 5b contains the best preserved chondrules with the least amount of altered chondrule glass, whereas specimen 11i is devoid of any well preserved chondrules and contains abundant framboidal magnetite clusters. All specimens also have variable proportions of lithic fragments. Here we expand on our previous efforts and investigate whether the macroscopic variations are mirrored at the sub-micron level in the matrix of each sample. Such observations can add an additional parameter in establishing an overall mineralogical framework for determination of the degrees of alteration in the Tagish Lake meteorite (TL).

**Samples and Methodology:** We examined specimens 5b, 11i, and 11h, representing the range of macroscopic variation within the pristine TL suite [3,4]. An FEI Nova 600 focused ion beam scanning electron microscope (FIB-SEM) at the Naval Research Laboratory (NRL) was used to make electron-transparent cross-sections (~10  $\mu\text{m}$  wide) using previously described methods [5]. A total of four FIB sections were made from polished probe mounts: one each from 5b and 11h, and two from 11i (one from the matrix and one from a lithic clast). All FIB sections were examined at NRL with a 200 keV JEOL 2200FS transmission electron microscope (TEM) equipped with an energy-dispersive X-ray spectrometer (EDS) and scanning-TEM (STEM) based bright- and high-angle annular-dark-field detectors (HAADF).

**Observations:** *5b Matrix:* The sample contains areas of amorphous groundmass and pores held together by epoxy. The porosity is thought to be primary [1]. Some areas of the groundmass contain poorly ordered, ribbon-like silicate structures (8-15 nm wide by 120 nm long on average) and fine-grained sulfides of various shapes, e.g., spheres and rods (~100- to 200-nm wide, respectively). The morphology of the ribbon-like structures suggests that these are sheet silicates. Large subhedral to anhedral sulfides (1-3  $\mu\text{m}$  wide) also occur in isolated domains. The section contains a large

Ca-rich carbonate grain (3  $\times$  4  $\mu\text{m}$ ) identified through EDS and selected-area electron-diffraction (SAED) patterns. The carbonate grain is irregular in shape and possibly consists of several sub-grains.

*11h Matrix:* There is an overall decrease in porosity across the 11h section, and some parts of it resemble the porosity of the 5b matrix. The sample is enriched in numerous sulfides and carbonate grains. Some sulfides concentrate in large (2-3  $\times$  0.5-1  $\mu\text{m}$ ) bands. The sulfide bands and carbonate grains are surrounded by amorphous material intermixed with rare sinuous sheet silicates. The middle part of the section is more compact and enriched in ribbon-like phyllosilicates. Although this middle part is devoid of sulfide grains, a sulfide/oxide circular rim with a diameter of ~ 4-5  $\mu\text{m}$  surrounds this more compact, phyllosilicate-rich area. Within it occurs a large (1  $\times$  0.5  $\mu\text{m}$ ) grain identified through spectral imaging to be enriched in P, Ni and Fe (possibly schreibersite or a phosphate, but the thickness of the grain made SAED difficult). One side of this grain appears to be embayed by phyllosilicates whereas the opposite side has a distinct boundary with the sheet silicates.

Several carbonate grains are present in this section. One grain has a circular shape with a partially hollow core contains in sulfides. HAADF imaging shows concentric contrast variations throughout the grain. EDS spectral imaging indicates that the outside of this carbonate grain is enriched in Mg and Ca, whereas the partially hollow core is enriched in Fe with minor Mn, which may suggest a change in the fluid chemistry with the grain growth (Fig.1).

*11i Matrix:* We made two 11i sections, 11i-1 and -2. Section 11i-1 was extracted from the part of the matrix that appears dark and porous on the macroscopic scale in back-scattered electron images, which we interpret as representative of typical 11i matrix. On the TEM scale, this section contains unevenly distributed sulfides (bands and patches), most of which have sub-hedral morphologies (up to 1.2  $\mu\text{m}$ ) but minor rods (up to 0.5  $\mu\text{m}$ ) also occur. The areas devoid of sulfides contain only sheet silicates, which exhibit sinuous textures, and which high-resolution TEM (HRTEM) reveals have varied degrees of order. Measurements of HRTEM images of ordered regions reveal lattice-fringe spacings of 0.10-0.11 nm, consistent with saponite, and up to 0.14 nm, suggesting serpentine integrown with a chlorite-type phase. Similar phyllosilicate types have been observed in previous studies

[e.g., 2,6]. The section also contains two large Ca-rich carbonate grains ( $\leq 3 \times 1.5 \mu\text{m}$ ) and several euhedral to rod-shaped olivine grains. Overall, this matrix section is highly porous with large cavities (several microns wide) of epoxy devoid of any minerals, i.e., its porosity is similar to 5b and also believed to be primary based on our observations.

Section 11i-2 was made from a lithic fragment. Lithic fragments are clearly seen on the macroscopic scale as more compact objects with relatively higher contrast in back-scattered electron images. On the TEM scale this section contains a compact area at the top, composed entirely of phyllosilicates with a flower-like texture (Fig. 2). This morphology has a compact core (diameters range from  $\sim 0.3$  to  $1 \mu\text{m}$ ) composed of sulfides and phyllosilicates curled onto each other from which grains of sheet silicates radiate ( $0.05 \times 0.4 \mu\text{m}$ ). Sheet silicates in the core and those radiating from it have 0.7-nm basal spacing, corresponding to serpentine. The origin of the ‘flower’ serpentine is unclear at the present. The lower part of this section is enriched in sulfides and has a porous texture, similar to the FIB section of 11i-1. There is a large silicate grain on the boundary between the compact, phyllosilicate-rich and the more porous areas. Part of the silicate grain ( $200 \times 300 \text{ nm}$ ) is embayed on both sides by phyllosilicates. A fractured nanoglobule [6], surrounded by fine-grained and ropey phyllosilicates, occurs near the base of this FIB section.

**Summary:** The mineralogy of the three matrix samples is similar. All contain phyllosilicates with various degrees of order, identified as mostly saponite and serpentine with sinuous textures and sometimes intermixed with amorphous material; large (up to  $3 \mu\text{m}$ ) carbonate grains; and minor olivines. Fe-Ni sulfides are present in all samples; however, their abundance and shapes varies. For example, the 5b matrix contains more rod-shaped sulfides than other samples, whereas 11h matrix has relatively large bands of sulfide enrichments. We also note two significant observations. The first is the prominent serpentine ‘flower’ texture in 11i-2 FIB section, which could give clues to the growth conditions (e.g., T, P) of this mineral [7]. And the second observation is the apparent inverse relationship between porosity and phyllosilicate abundance. For example, the lithic fragment from the 11i specimen (11i-2 FIB section), which is more compact than the rest of the matrix on both sub-micron TEM and micron SEM scales, is also composed entirely of phyllosilicates. This suggests that lithic fragments of 11i could have experienced higher degrees of aqueous alteration than the rest of the matrix.

**Acknowledgements:** This study was supported by the Carnegie Institution of Canada grant to Larry Nit-

tlar, NASA Origins grant NNH10AO16I to TJZ and RMS, Natural Sciences and Engineering Research Council of Canada grant 261740 to CDKH, and CGS D3 NSERC and AI doctoral scholarships to AB.

**References:** [1] Brown P.G. et al. (2002) *Meteoritics and Planetary Science*, 37(5), 661-675. [2] Zolensky et al. (2002) *Meteoritics and Planetary Science*, 37(5), 737-761. [3] Blinova et al. (2009) *LPSC XL*, Abstract #2039. [4] Blinova et al. (2010) *LPSC 41<sup>st</sup>*, Abstract #2140. [5] Zega T. et al. (2007) *Meteoritics and Planetary Science*, 42, 1373-1386. [6] Nakamura K. (2002) *International J of Astrobiology*, 1(3), 179-189. [7] Wicks F.J. and Wittaker E.J.W. (1977) *Canadian Mineralogist*, 15, 459-488.

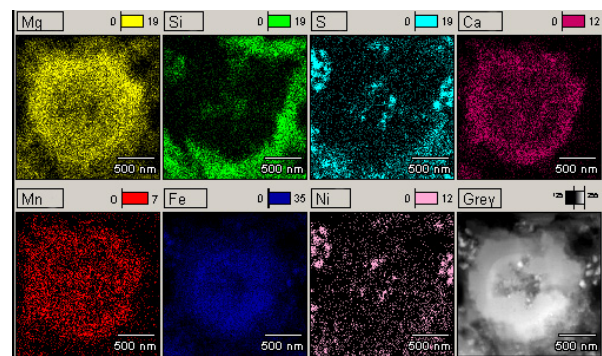


Figure 1: Spectral image of the circular carbonate grain from 11h matrix.

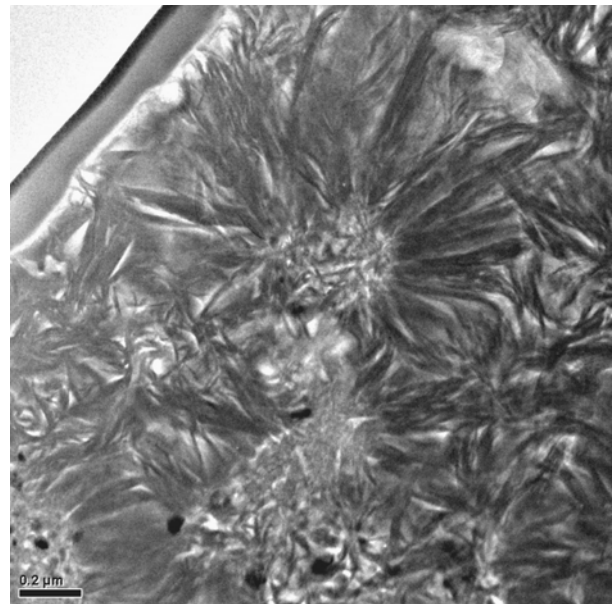


Figure 2: ‘Flower’ texture in section 11i-2.